MedChemComm

Accepted Manuscript

ROYAL SOCIETY OF CHEMISTRY

www.rsc.org/medchemcomm

Cite this: DOI: 10.1039/c0xx00000x

www.rsc.org/xxxxxx

CONCISE ARTICLE

Design, synthesis and anticancer mechanistic studies of linked azoles

Md. Amirul Islam,[a] Yuqi Zhang,[a] Yao Wang,[a] and Shelli R. McAlpine*[a]

Received (in XXX, XXX) XthXXXXXXXXX 20XX, Accepted Xth XXXXXXXXX 20XX
DOI: 10.1039/b000000

Herein we report the synthesis and biological activity evaluation of 2, 4 linked azole-containing molecules. A total of 13 linked thiazole- and oxazole-containing compounds were synthesized in good yields. Cytotoxicity evaluation of those compounds showed that they have low-micromolar anticancer potency against HCT116 colon cancer cells. Mechanism of action investigation studies indicated that linked thiazoles were significantly more biologically active than the corresponding oxazole-containing molecules in inducing apoptotic cancer cell death. Incorporation of a stereocenter at an azole end and an amide cap at the other end provided a compound that induces DNA damage and leads to G2/M cell cycle arrest and activation of the G2/M DNA damage checkpoint.

Introduction

Heterocycles play a prominent role in the biological activity of natural products.[1-8] Incorporating heteroatoms into a molecular scaffold increases the drug-like properties of molecules, providing solubility, hydrogen bonding, and rigidity. The presence of electron lone pairs on heteroatoms means that they readily form hydrogen bonding with water, which increases their solubility, and improves binding to their biological target thereby enhancing the potency of a molecule.[9] The limited number of rotatable bonds in heterocyclic compounds makes them structurally rigid, optimizing binding interactions and decreasing their degradation by proteolytic enzymes. Moreover, the ability of heterocycles to interact with a biological target via π-stacking opens new opportunities for binding sites.[10] The most common heterocycles that are present in biologically active natural products are thiazoles and oxazoles. The presence of these two heterocycles in a number of diverse molecular scaffolds makes them structurally and biologically interesting.

Urukthapelstatin A (Ustat A) (**Figure 1**) is a natural product isolated from marine bacteria and it shows potent anticancer activity against a panel of human cancer cell lines with an average IC_{50} value of 12 nM.[11-13] This molecule has a unique bisoxazole and bisthiazole moiety located within the macrocycle. HXDV (**Figure 1**) is a synthetic derivative of telomestatin, which exhibits anti-proliferative and apoptotic activity by stabilizing G-quadruplex, thereby inducing M-phase cell cycle arrest.[14-15] It has two linked tri-oxazoles within its macrocyclic backbone. Marthiapeptide A (**Figure 1**) is another potent natural product that contains a linked trithiazole-thiazoline system, and cytotoxicity with an IC_{50} = ~380-520 nM against a panel of cancer cell lines.[16]

Inspired by the linked azoles observed within these three biologically active molecules (Ustat A, HXDV, and Marthiapeptide A) and the activity of linked azole molecules previously reported[12, 13, 17-20] we designed a series of short fragments that investigated whether stereochemistry impacted the heterocyclic portion of the fragment (**Figure 2**). Starting with either an R and S stereochemical orientation of the methyl moiety and then capping the fragment with 3 different moieties (ester, amide, thioamide) showed that both the stereochemistry and the capping moiety made a significant difference to the biological activity of the compound. Testing the cytotoxicity of these compounds against colon cancer cell lines and evaluating their mechanism of action lead to a set of conclusions. First, linked thiazoles have significantly higher biological activity than linked oxazoles. Second, the most effective sequence is three linked

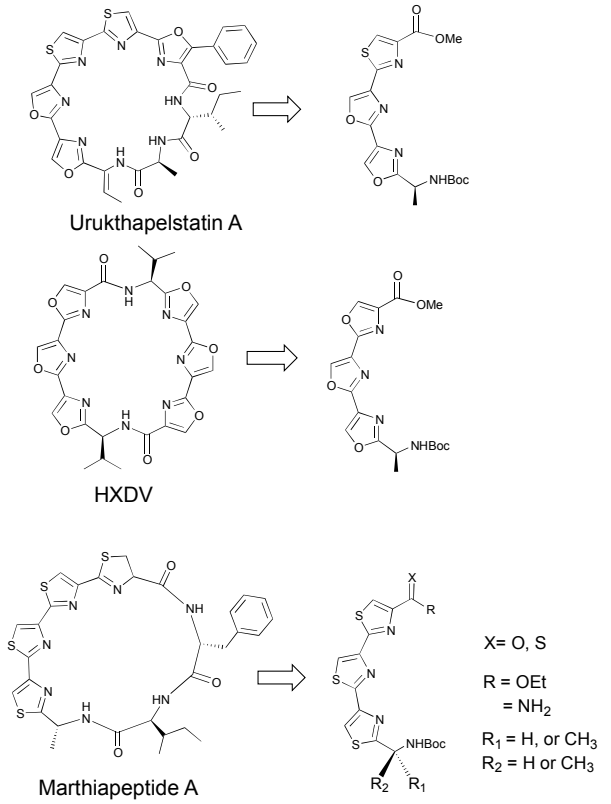

Figure **1.** Heterocyclic fragments of three anticancer molecules that contain linked oxazoles and thiazoles.

thiazoles, where fewer linked thiazoles are less active. Third, the stereochemistry of the starting alanine alters the activity of the compound, with the S enantiomer being more effective than R. Finally, the capping moiety makes a significant difference in the molecules biological activity, with the amide-capping moiety being the most active structure in cytotoxicity, apoptosis, cell cycle, and DNA damage assays.

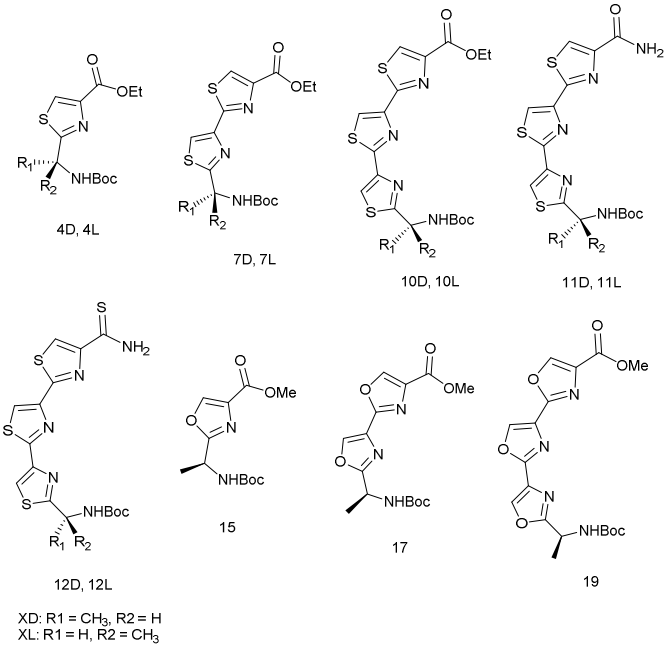

Figure 2. Design of linked azole-containing molecules.

Results and Discussion

Several methods have been reported for the synthesis of thiazoles and oxazoles.[20-24] Employing a modified Hantzsch reaction, which involves condensation of α-haloketone with thioamide derivatives, we generated the linked thiazoles (Scheme 1).[25-28] The synthesis started with tert-Boc protected D- or L-alanine carboxylic acid. The amino acid was converted to its methyl ester using trimethylsilyldiazomethane (TMSD) in a mixture of methanol and benzene and the ester was subjected to amide formation using an ammonia hydroxide solution in a protic solvent. The amide (**2**) was reacted with Lawesson's reagent to furnish Thioamide (**3**). The thioamide was then subjected to a modified Hantzsch reaction using ethylbromopyruvate and $KHCO_3$ to form a hydroxyl thiazoline intermediate. The thiazoline was then dehydrated using trifluoroacetic anhydride (TFAA) and pyridine to form the monothiazole **4** in good yield (74% for 2 steps)[29]

Amination of **4** was accomplished using an ammonia solution, and then subsequent formation of the thioamide (**6**) was achieved using Lawesson's reagent. Formation of the hydroxyl thiazoline using the modified Hantzsch conditions and subsequent dehydration of thiazoline yielded **7** (70% for 2 steps). Repeating this process we generated compound **10** with a 70% yield. Amination of **10** generated **11** and treatment of the amide with Lawesson's reagent resulted in **12** (62%).

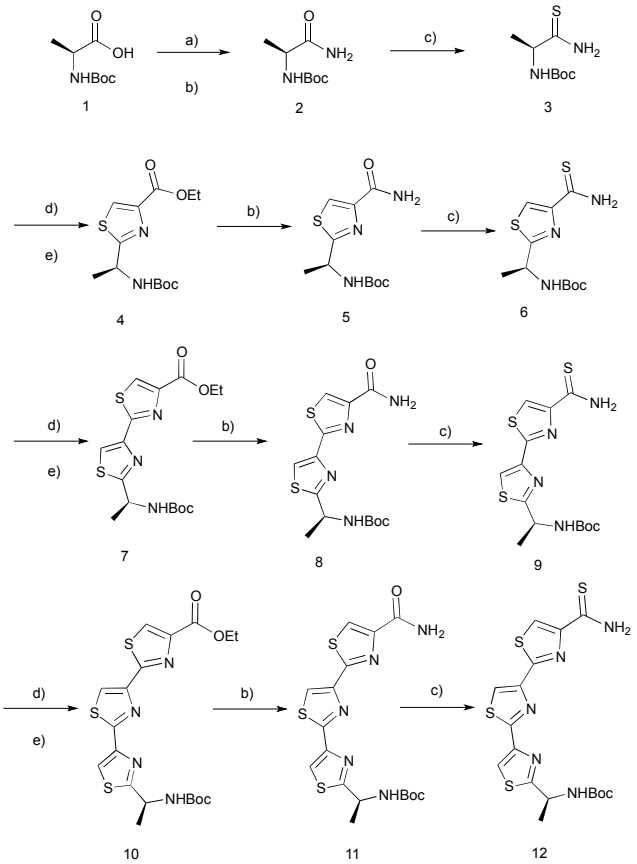

Scheme 1. Synthesis of linked thiazoles. Conditions: a) TMSD, Benzene/MeOH (3:1, 0.1 M), quant. yield. b) NH_4OH/MeOH (1:1, 0.05 M), quant. yield. c) Lawesson's Reagent (0.75 eq), THF (0.05 M), 68% for **3**, 65% for **6**, 62% for **9** and **12**. d) $KHCO_3$ (8 eq), DME (0.05 M), rt, $BrCH_2COCO_2Et$ (3 eq), 16 h. d) TFAA (4 eq), Pyridine (9 eq), DME (0.05 M); then TEA (2 eq), 0°C to rt, 74% for **4**, 70% for **7** and **10** (over 2 steps).

Generating linked oxazoles was accomplished via cyclization and oxidation of serine (Ser) containing peptides (**Scheme 2**).[6] Boc-Serine (Bn) was converted to its methyl ester using TMSD. Deprotection of the amine was done using TFA and the free amine was subsequently coupled with free acid Boc-Ala-OH to form the dipeptide precursor using 2-(1H-benzotriazol-1-yl)-1,1,3,3-tetramethyluronoium hexafluorphosphate (TBTU) and diisopropylethylamine (DIPEA). The benzyl protecting group was removed by hydrogenation with Pd/C to generate compound **14**, which then underwent an intramolecular cyclization using the fluorinating agent diethylaminosulfur trifluoride (DAST) to form the intermediate oxazoline. The oxazoline was subsequently oxidized using $BrCCl_3$ and the hydroxyl moiety eliminated using 1,8-diazabicyclo[5.4.0]undec-7-ene (DBU) to produce **15** with an excellent yield (83%). Compound **15** was treated with LiOH to generate the free acid, which was subsequently coupled with free amine NH_2-Ser(Bn)-OMe to obtain **16**. Deprotection of the alcohol and formation of the oxazole resulted in **17** (83% for 3 steps). Finally, hydrolysis of the ester on **17**, coupling with serine, deprotection of the alcohol and formation of oxazole generated **19** (78% for 3 steps).

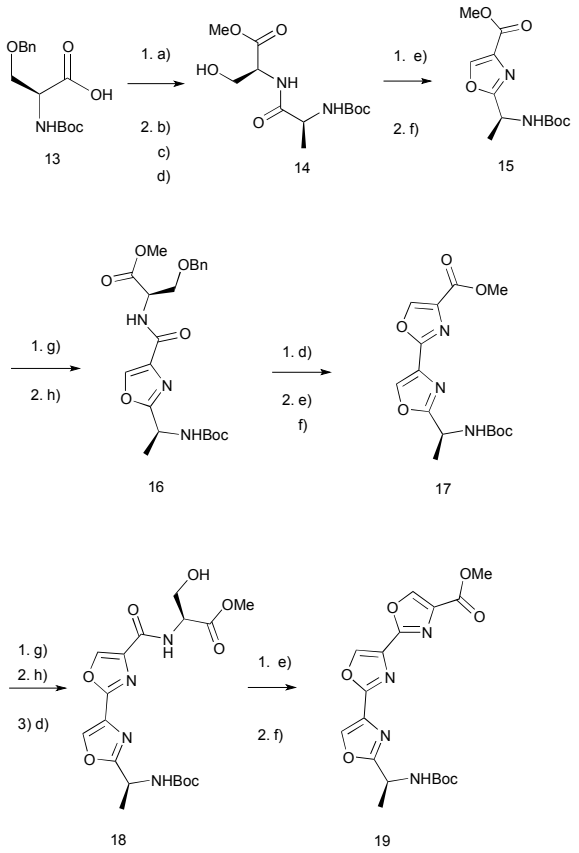

Scheme 2. Synthesis of linked oxazoles. Conditions: a) MeOH/Benzene (1:3, 0.1 M), TMSD (3.0 eq). b) TFA/CH_2Cl_2 (1:4, 0.1 M), Anisole (2.0 eq). c) Boc-Ala-OH (1.1 eq), TBTU (1.1 eq), DIPEA (8.0 eq), CH_2Cl_2 (0.1 M). d) H_2 (1 atm), Pd/C, EtOH (0.1 M). e) DAST (1.1 eq), K_2CO_3 (2.0 eq), CH_2Cl_2 (0.1 M), -78ºC. f)DBU (2.0 eq), $CBrCl_3$ (2.0 eq), CH_2Cl_2 (0.1 M), -47ºC. g) LiOH (8.0 eq), MeOH (0.1 M). h)H-Ser(Bn)-OMe (0.9 eq), TBTU (1.1 eq), HATU (1.1 eq), DIPEA (10 eq), CH_2Cl_2 (0.1 M).

Structure-activity relationships

The synthesized thiazole and oxazole molecules were tested at 50 μM in a cytotoxicity assay (CCK-8), where we evaluated their activity against colon cancer cell line HCT116 (**Figure 3**).[30] As is evident in the graph, the tri-thiazoles (compounds **10-12**) are significantly more active than the oxazoles series.

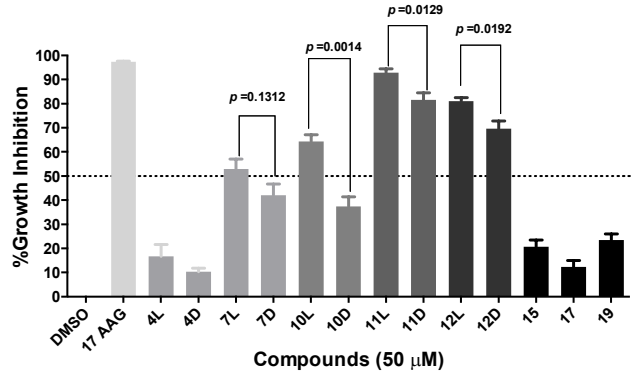

Figure 3. Growth inhibition of compounds at 50 μM. Percentage growth inhibition of treated HCT116 cells was measured using a CCK8 assay. Data is from three separate experiments performed in quadruplicate and the error bars are the standard errors of the mean (SEM). (*P* values were calculated using Graph pad Prism version 6).

Furthermore, the L-alanine series (S- stereochem: **10L- 12L**) is consistently more active than the D-alanine series (**10D-12D**). Thus, the stereochemistry of the methyl moiety must be impacting the planarity of the compound and hence its mechanism of action. We also determined the IC_{50} values of compounds that showed growth inhibition more than 70% at 50 μM concentrations (**11L**, **11D**, **12L**, and **12D)**. We found that **11L** is the most potent compound having IC_{50} value of 7.64 μM against HCT116 cells (**Table 1**).

Table 1. IC_{50}* values of potent compounds (μM) against HCT116 cancer cells

Compounds	11L	11D	12L	12D
IC_{50} (μM)	7.6 ± 1.0	22.4 ± 1.6	38.1 ± 2.6	45.2 ± 2.1

*IC_{50} values of **11L**, **11D**, **12L**, and **12D** with their standard error of mean (SEM) against colon cancer cell line HCT116 using CCK-8 assay. Data represents results from a concentration curve taken from six concentrations, where each concentration data point is from three separate experiments performed in quadruplicate. Concentration curves are available in supplementary material.

Mechanistic studies

Performing an apoptosis analysis using Annexin-V/7-AAD cytofluorometric staining supported the IC_{50} data, where **11L** was more potent than **11D** at inducing apoptotic cancer cell death (**Figure 4a**). Compared to the control treatment (DMSO), over 60% of HCT116 cells undergo apoptosis after 30 hrs of incubation with **11L** (30 μM) (versus 30% under the same conditions with **11D)**. Treatment of HCT116 cells with **11L** for 20 hrs significantly increased the population of living cells in G2/M phase with a decrease in both G0/G1 and S phases, compared to the control treatment (**Figure 4b**). These data indicate that **11L** induces a G2/M arrest in HCT116 cells.

Since many chemotherapeutic agents arrest cancer cells in G2/M phase by causing DNA damage, we examined if **11L** also induced DNA damage in HCT116 cells and if such damage happens in a specific cell cycle phase. This was done by flow cytometry detecting the phosphorylation of histone H2AX on serine 139 (γ-H2AX), which is a prominent marker of DNA damage,[31] while measuring DNA content with propidium iodide. We found that in the treatments with **11L** or **11D** γ-H2AX formed at all cell cycle phases, although with a significant preference for S and G2/M phases (**Figure 4c**). Similar effects were observed in the Paclitaxel (Pac) and Doxorubicin (Dox) treatments. Comparison to both Pac and Dox showed that **11L** was more effective at inducing DNA damage than either of these anticancer agents when cells were treated at their respective IC_{50} values. Those results indicated that **11L** and **11D** triggered apoptosis in HCT116 cells through causing DNA damage, although **11L** is more effective than **11D** in all cases. This damage manifested primarily in the G2/M cell cycle arrest

Based on the previous observations in cell cycle analysis and DNA damage detection, we speculated that **11L** triggered apoptosis in HCT116 cells possibly by activating the G2/M checkpoint. In response to many types of DNA damage, cells

activate powerful DNA damage-induced cell cycle checkpoints that coordinate cell cycle arrest with recruitment and activation of DNA repair machinery.[32-34] If cells fail to repair the damage in a certain time period, pathways involved in programmed cell death will be initiated, leading to the elimination of irreparably damaged cells by apoptosis.[32, 35] In order to prove our hypothesis, we measured the population changes of mitotic cells (cells at M phase) caused by drug treatments. Results are shown as the mitotic index, which represents the percentage of mitotic cells in the total population (**Figure 4d**, the index of DMSO control was considered as 1). If the G2/M checkpoint is activated, we should see a decrease in the population of M phase cells, that is, a decrease in the mitotic index. Mitotic cells were determined and distinguished from the entire population by flow cytometry. Detection of the phosphorylated Histone H3 while measuring DNA content with propidium iodide was used as it is an ideal indicator of mitotic cells. Specifically, Histone H3 is phosphorylated during mitosis.[36] Our results showed that **11L** reduced the mitotic index in a time- and concentration-dependent manner (**Figure 4d**). Contrary to the control compound Paclitaxol, which traps cells in M phase (indicated by the dramatic increase of mitotic index), **11L** arrests cells in G2 phase, which is similar to the effect caused by Doxorubicin (**Figure 4d**). Combined, those data demonstrated that **11L** triggered apoptotic cancer cell death by causing DNA damage, and leads to G2/M cell cycle arrest and the activation of a G2/M DNA damage checkpoint.

a)

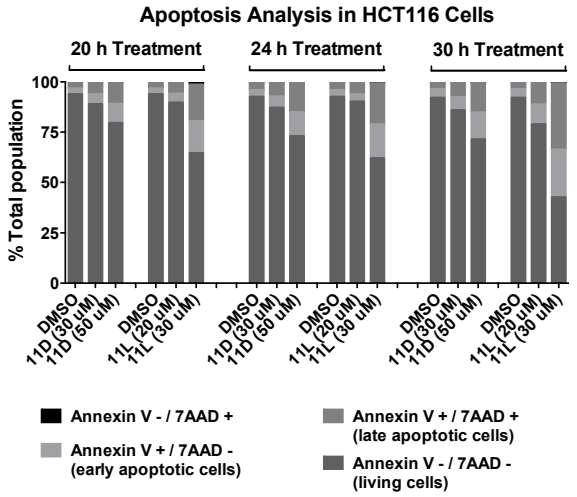

b)

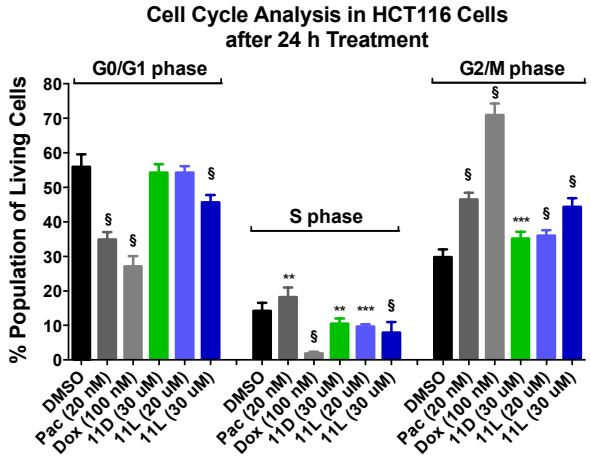

c)

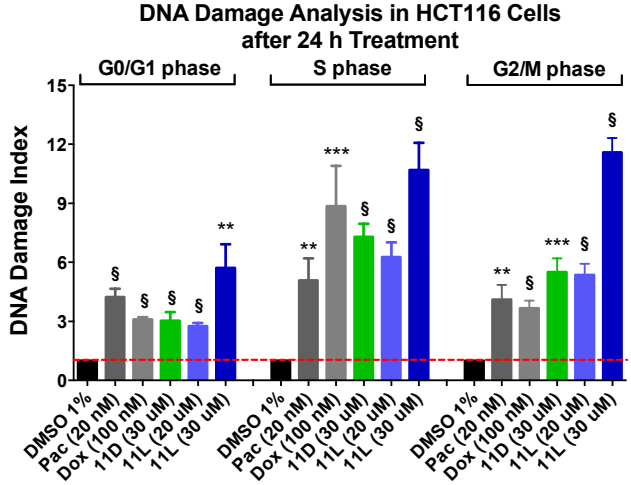

d)

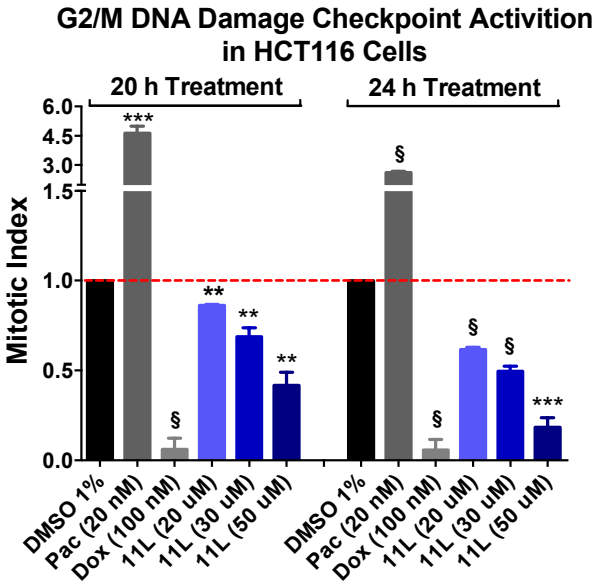

Figure 4. The effects of **11L** and **11D** on apoptosis, cell cycle progression, and DNA damage response in HCT116 cells. a) After indicated treatments cells were stained with Annexin V-FITC/7AAD and analysed by flow cytometry for apoptosis analysis. b) After indicated treatments cells were stained with PI for cell cycle analysis by flow cytometry. The percentages of cells in the G0/G1, S, and G2/M phases of cell cycle are indicated in bar graphs. c) Treatments with **11D** and **11L** for 20 or 24 h resulted in DNA damage in HCT116 cells. Treated cells were stained with DNA damage marker γ-H2AX and analysed by flow cytometry. d) Treatment with **11L** for 20 or 24 h activated the G2/M DNA damage checkpoint in HCT116 cells. Treated cells were stained with Histone H3 (phospho, Ser-10)/PI and analysed by flow cytometry. All values presented are average ± SEM of at least three independent experiments. Differences between indicated data and DMSO control are represented with *P* values (*, $P < 0.05$; **, $P < 0.01$; ***, $P < 0.005$; and §, $P < 0.001$).

Conclusions

In conclusion, we have shown that linked thiazoles have significantly higher biological activity than linked oxazoles, with the most effective sequence being three linked thiazoles. A single stereocenter on the otherwise flat molecule alters the activity of the compound and indicates that the molecule is binding to a chiral target. The capping moiety makes an important contribution to the biological activity, with the amide being the most effective cap for these molecules. Recent work by Wipf and co workers[37] shows that alcohol capping groups generate compounds that have nanomolar IC_{50} values, thus, our hypothesis is that our compounds might have improved potency if they were converted to an alcohol. In addition, Wipf's work suggests that the N-Boc protecting group on our molecules may be coming off once the molecule has entered the cell, generating the free amine as the active compound. Mechanistic investigation shows that the most effective molecule, **11L**, induces apoptosis in over 60% of HCT116 cells within 30 hrs of treatment, which is significantly higher than **11D** (25%). The G2/M cell cycle arrest and the DNA damage-induced G2/M checkpoint activation caused by **11L** indicate that its mechanism of action in inducing apoptosis is associated with the pathways involved in DNA damage and repair response. The loss of DNA damage checkpoints during early stages of tumorigenesis facilitates acquisition of additional mutations, and is an optimal mechanism that is frequently exploited in chemotherapies. Given that **11L** is more effective than **11D** in causing DNA damage-induced G2/M cell cycle checkpoint and apoptosis at the same concentrations, the stereocenter must be play an important role in the events associated with DNA damage and repair pathways. These findings have implications for synthesizing derivatives of heterocyclic-containing natural products and in designing fragments of the heterocyclic portions of the compounds.

Acknowledgements

We thank the University of New South Wales for a tuition fee waiver to A.I. and Y.W. We thank NHMRC APP1043561 for support on this project.

Notes

[a]*School of Chemistry, 219 Dalton, Gate 2 High Street, University of New South Wales, Sydney, NSW, 2052, Australia. Fax: +61-2-9385-4000 Tel: +61-4-1672-8896; E-mail:s.mcalpine@unsw.edu.au*

† Electronic Supplementary Information (ESI) available: synthetic procedures spectra for the intermediates and final structures of all molecules. Details of biological assays are also included. See DOI: 10.1039/b000000x/

References

1. M. Baumann, I. R. Bazendale, S. V. Ley and N. Nikbin, *Beilstein J. Org. Chem.*, 2011, **7**, 422-495.
2. D. L. Boger, *Patent application: PCT/US2007/019471/ US2010/0075931 A1*, 2012, **12/310,474**.
3. Q. Dang, L. Yan, D. K. Cashion, S. R. Kasibhatla, T. Jiang, F. Taplin, J. D. Jacintho, H. Li, Z. Sun, Y. Fan, J. DaRe, F. Tian, W. Li, T. Gibson, R. Lemus, P. D. van Poelje, S. C. Potter and M. D. Erion, *J. Med. Chem.*, 2011, **54**, 153-165.
4. P. I. Dosa, J. C. Ruble and G. C. Fu, *J. Org. Chem.*, 1997, **62**, 444-445.
5. M. Duchler, *J. Drug Target.*, 2012, **20**, 389-400.
6. R. A. Hughes and C. J. Moody, *Angewandte Chemie International Edition*, 2007, **46**, 7930-7954.
7. B. Wagner, D. Schumann, U. Linne, U. Koert and M. A. Marahiel, *J. Am. Chem. Soc.*, 2006, **128**, 10513-10520.
8. K. Sivonen, N. Leikoski, D. P. Fewer and J. Jokela, *Appl. Microbiol. Biotechnol.*, 2012, **86**, 1213–1225.
9. A. Gomtsyan, *Chem. Heterocycl. Compd.*, 2012, **48**, 7-10.
10. M. Ma, Y. Cheng, Z. Xu, P. Xu, H. Qu, Y. Fang, T. Xu and L. Wen, *European Journal of Medicinal Chemistry*, 2007, **42**, 93-98.
11. y. Matsuo, K. Kanoh, H. Imanaka, K. Adachi, M. Nishizawa and Y. Shizuri, *J. Antibiot.*, 2007, **60**, 256-260.
12. C.-C. Lin, W. Tantisantisom and S. R. McAlpine, *Org. Lett.*, 2013, **15**, 3574-3577.
13. S.-J. Kim, C.-C. Lin, C.-M. Pan, D. P. Rananaware, D. M. Ramsey and S. R. McAlpine, *Med. Chem. Comm.*, 2013, **4**, 406-410.
14. Y.-C. Q. Tsai, H.; Lin, C.-P.; Lin, R.-K.; Kerrigan, J. E.; Rzuczek, S. G.; LaVoie, E. J.; Rice, J. E.; Pilch, D. S.; Lyu, Y. L.; Liu, L. F., A *J. Bio. Chem.*, 2009, **284**, 22535-22543.
15. M. R. Satyanarayana, S. G.; LaVoie, E. J.; Pilch, D. S.; Liu, A.; Liu, L. F.; Rice, J. E., , *Bioorg. Med. Chem.*, 2008, **18**, 3802-3804.
16. X. Zhou, H. Huang, Y. Chen, J. Tan, Y. Song, J. Zou, X. Tian, Y. Hua and J. Ju, *J. Nat. Prod.*, 2012, **75**, 2251-2255.
17. H. Wahyudi, W. Tantisantisom and S. R. McAlpine, *Tetrahedron Lett.*, 2014, **55**, 2389-2393.
18. W. Tantisantisom, D. M. Ramsey and S. R. McAlpine, *Org. Lett.*, 2013, **15** 4638-4641.
19. H. Wahyudi, W. Tantisantisom, X. Liu, D. M. Ramsey, E. K. Singh and S. R. McAlpine, *J. Org. Chem.*, 2012, **77**, 10596-10616.
20. E. Singh, D. M. Ramsey and S. R. McAlpine, *Org. Lett.*, 2012, **14**, 1198-1201.
21. M. R. Davis, E. K. Singh, H. Wahyudi, L. D. Alexander, J. Kunicki, L. A. Nazarova, K. A. Fairweather, A. M. Giltrap, K. A. Jolliffe and S. R. McAlpine, *Tetrahedron*, 2012, **68**, 1029-1051.
22. N. U. Güzeldemirci and Ö. Küçükbasmacı, *European J. Med. Chem.*, 2010, **45**, 63-68.
23. J. P. Marino, P. W. Fisher, G. A. Hofmann, R. B. Kirkpatrick, C. A. Janson, R. K. Johnson, C. Ma, M. Mattern, T. D. Meek, M. D. Ryan, C. Schulz, W. W. Smith, D. G. Tew, T. A. Tomazek, D. F. Veber, W. C. Xiong, Y. Yamamoto, K. Yamashita, G. Yang and S. K. Thompson, *J. Med. Chem.*, 2007, **50**, 3777-3785.
24. B. Soni, M. S. S. Ranawat, Rambabu, A. Bhandari and S. Sharma, *Eur. J. Med. Chem.*, 2010, **45**, 2938-2942.

25. K. M. Aitken and R. A. Aitken, *Tetrahedron*, 2008, **64**, 4384-4386.
26. M. Narender, M. S. Reddy, R. Sridhar, Y. V. D. Nageswar and K. RamoRao, *Tetrahedron Letters*, 2005, **46**, 5953-5955.
27. T. M. Potewar, S. A. Ingale and K. V. Srinivasan, *Tetrahedron*, 2007, **63**, 11066-11069.
28. E. Aguilar and A. I. Meyers, *Tetrahedron Lett*, 1994, **35**, 2473-2476.
29. C.-M. Pan, C.-C. Lin, S. J. Kim, R. P. Sellers and S. R. McAlpine, *Tetrahedron Lett.*, 2012, **53**, 4065-4069.
30. H. Ohori, H. Yamakoshi, Tomizawa M, Shibuya M, Kakudo Y, Takahashi A, Takahashi S, Kato S, Takao T, Ishioka C, Iwabuchi Y and S. H., *Mol. Cancer. Ther.*, 2006, **5**, 2563-2571.
31. E. L. Davenport, H. E. Moore, A. S. Dunlop, S. Y. Sharp, P. Workman and G. J. Morgan, *Blood*, 2007, **110**, 2641-2649.
32. M. V. Powers and P. Workman, *FEBS Lett*, 2007, **581**, 3758-3769.
33. E. L. Davenport, G. J. Morgan and F. E. Davies, *Cell Cycle*, 2008, **7**, 865-869.
34. C. S. Mitsiades, N. S. Mitsiades, C. J. McMullan, V. Poulaki, A. L. Kung and F. E. Davies, *Blood*, 2006, **107**, 1092-1100.
35. E. Y. Komarova, E. A. Afanasyeva, M. M. Bulatova, M. E. Cheetham, B. A. Margulis and I. V. Guzhova, *Cell Stress Chaperones*, 2004, **9**, 265-275.
36. M. V. Powers, P. A. Clarke and P. Workman, *Cancer Cell*, 2008, **14**, 250-262.
37. J. Salamoun, S. Anderson, J. C. Burnett, R. Gussio and P. Wipf, *Org. Lett.*, 2014, **16**, 2034-2037.